CHAPTER 3 Modeling Electromagnetic Properties of Soils

3.1 Introduction

Most soils encountered in engineering practice contain both clay and nonclay materials. The electromagnetic properties of a two-phase mixture of nonclay minerals and water can be analyzed using many empirical or theoretical formulas (Sen et al. 1981; Sihvola 1999) because sand particles have inert surfaces which usually do not react with pore fluids. However, the presence of clay materials greatly complicates the responses of a soil in an electromagnetic field because the electromagnetic properties of clay minerals can be affected by many factors including the particle size (O'Konski 1960; Schwarz 1962), particle shape and orientation (Fricke 1953; Jones and Or 2003), specific surface area (Jones and Or 2002), temperature (Chen et al. 1999; Or and Wraith 1999; Chen and Or 2006) and pore fluid chemistry (Friedman 2005).

As shown in the previous chapter, the dielectric dispersion in the 1MHz to 1 GHz frequency range is primarily attributed to the interfacial polarization (Maxwell-Wagner effect) and bound water relaxation. Several approaches are available to interpret the dielectric dispersion behavior caused by the interfacial polarization, including the three-path model by Sachs and Speigler (1964), the theoretical model developed by Thevanayagam (1995) and the impedance spectroscopy (IS) techniques proposed by Rinaldi and Francisca (1999). Each model has a set of parameters. The values of these parameters are determined by fitting theoretical models to the measured dielectric dispersion spectra. Rinaldi and Francisca (1999) showed that all three theoretical models

can give satisfactory fitting for the measured dielectric dispersion spectra, but the soil compositional and structural characteristics interpreted by each model were different. This indicated that the soil properties obtained by curve fitting techniques may differ from their true values even if the perfect fitting is achieved. The curve fitting techniques alone can not guarantee the correct estimation of soil composition and structure because (1) the idealized model may not match the true structure of a soil; (2) some parameters have no clear physical meanings; (3) the solution is not unique and different combinations of parameters can give similar degree of fitting.

Despite many efforts to model the responses of soils in an EM field, our ability to deduce the components and structure of clayey soils from their electromagnetic properties is still limited because: (1) no model has provided a means to study the electromagnetic properties of a soil containing both clay and non-clay minerals; (2) clay particles were assumed to be electromagnetically isotropic and have constant dielectric permittivities, an assumption that may not be realistic; (3) dielectric permittivity and electrical conductivity were considered separately even though they are highly interrelated; (4) interfacial polarization and bound water polarization are treated separately despite the fact that they are coupled at frequencies lower than 1 GHz.

In this study, the dielectric permittivity and electrical conductivity of a sand-water mixture are calculated simultaneously by modifying the Maxwell-Garnett (MG) mixing formula. Secondly, a physically-based model is established to simulate the clay aggregates formed by stacked clay particles so that their electromagnetic properties can be determined, and then the electromagnetic properties of soils containing the aggregates can be calculated using the modified Maxwell-Garnett mixing formula. The model

establishes a framework through which the effects of both clay and non-clay minerals on the electromagnetic properties of a soil can be analyzed.

3.2 A New Theoretical Model

3.2.1 Maxwell-Garnett Mixing Formula

Many theoretical mixing formulas have been proposed to calculate the dielectric permittivity of a mixture from those of their components. Among them, the Maxwell-Garnett (MG) mixing formula (Maxwell Garnett 1904) is the most fundamental. It was developed for a two-phase mixture where spherical inclusions (particles) are scattered in a medium (pore fluids) as illustrated in Figure 3.1. The MG mixing formula was derived by combining the polarizability expression for a single spherical inclusion in a uniform field with the Clausius-Mossotti formula, which expresses the overall real permittivity of the mixture as a function of the polarizabilities of its components. The complete derivation can be found in Sihvola (1999). The mixing formula is expressed as:

$$\kappa_{mx}^{'} = \kappa_{en}^{'} + v \cdot \kappa_{en}^{'} \cdot \frac{\left(\kappa_{in}^{'} - \kappa_{en}^{'}\right)}{\kappa_{en}^{'} + N \cdot (1-v) \cdot \left(\kappa_{in}^{'} - \kappa_{en}^{'}\right)} \qquad [3.1]$$

where $\kappa_{mx}^{'}$ is the real permittivity of the mixture; $\kappa_{in}^{'}$ and $\kappa_{en}^{'}$ are the real permittivities of the inclusions and medium; v is the volumetric fraction of the inclusions; N is termed the depolarization factor, which characterizes how the shape and orientation of the inclusions affect the real permittivity of the mixture. For spheroidal inclusions, its value varies from 0 to 1. For spherical inclusions, N=1/3. The depolarization factor will be further discussed when clay-water mixtures are analyzed.

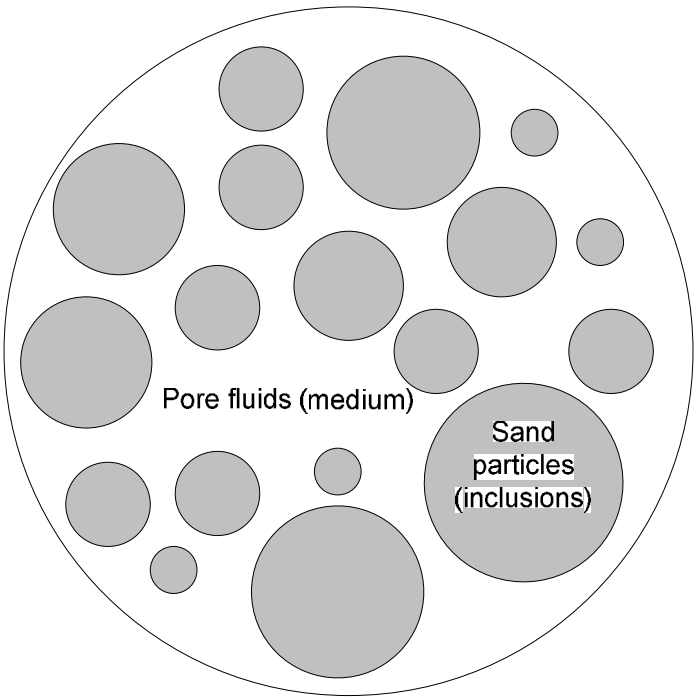

Figure 3.1 Spherical inclusions (particles) randomly distributed in a medium (pore fluids)

The MG mixing formula was originally derived for calculating the real permittivity of a mixture containing non-conductive particles. However, it also applies for conductive materials because the fundamental laws based on which the MG formula was derived also apply for the electrical conductivity (O'Konski 1960). In other words, the equivalent dielectric permittivity of a mixture can be calculated by substituting the real permittivities of both the inclusions and the medium in equation [3.1] with their equivalent dielectric permittivities κ_{en}^{*} and κ_{in}^{*}:

$$\kappa_{mx}^{*} = \kappa_{en}^{*} + v \cdot \kappa_{en}^{*} \frac{\left(\kappa_{in}^{*} - \kappa_{en}^{*}\right)}{\kappa_{en}^{*} + N \cdot (1-v) \cdot \left(\kappa_{in}^{*} - \kappa_{en}^{*}\right)} \qquad [3.2]$$

Although the MG mixing formula provides a convenient means to calculate the effective dielectric permittivity of a two-phase mixture, it may not be directly applied for

soil deposits because many soil deposits are densely packed, a condition that does not agree with an implicit assumption of the MG mixing formula, which requires that the concentration of the inclusions is sufficiently low so that the electromagnetic interferences among inclusions can be ignored. This problem can be approached by dividing the inclusions into small fractions and adding them to the medium (the bulk pore fluid) in a stepwise way, a procedure first introduced by Bruggeman (1935). Namely, the calculation of the mixture equivalent dielectric permittivity is an iterative process: the resulting equivalent dielectric permittivity from the addition of a small volume of particles is treated as a new medium for further addition of particles. The iteration process is formulated by modifying the equation [3.2] as:

$$\kappa^*_{en,i} = \kappa^*_{en,i-1} + v_i \cdot \kappa^*_{en,i-1} \cdot \frac{\kappa^*_{in} - \kappa^*_{en,i-1}}{\kappa^*_{in} + N \cdot (1 - v_i) \cdot \left(\kappa^*_{in} - \kappa^*_{en,i-1}\right)}, \quad \text{i} = 1, 2, \ldots \text{M.} \qquad [3.3]$$

in which $v_i = \dfrac{(v/M)}{\theta_w + i \cdot (v/M)}$

where θ_w is the volumetric water content of the bulk pore fluid; v is the volumetric fraction of the inclusions (particles), $v = 1 - \theta$; $\kappa^*_{en,i}$ and $\kappa^*_{en,i-1}$ are the equivalent dielectric permittivity before and after the i*th* fraction of inclusions v/M is added; the v_i is adjusted at each step because the total volume of the mixture increases when more particles are added. The initial value of the mixture equivalent dielectric permittivity is that of the bulk pore fluid, $\kappa^*_{en,0} = \kappa^*_{el}$. The mixture equivalent dielectric permittivity is obtained at the end of iteration $\kappa^*_{mx} = \kappa^*_{en,M}$. The above equation is named the modified MG mixing formula herein.

Since sand particles are approximately uni-dimensional, a sand-water mixture can be modeled as spherical sand particles (the inclusions) randomly distributed in the bulk pore fluid (the medium). To calculate the equivalent dielectric permittivity of the sand-water mixture, the equivalent dielectric permittivities of sand particles κ_s^* and the bulk pore fluid κ_{el}^* need to be determined.

3.2.2 Equivalent Dielectric Permittivities of Sand Particles and Bulk Pore fluid

The equivalent dielectric permittivities of both sand particles and pore fluid have three terms: the real permittivity κ', polarization loss κ'' and DC electrical conductivity σ_{dc}.

The polarization loss and DC electrical conductivity of sand particles are negligible. As a result, the equivalent dielectric permittivity of sand particles is approximately constant over the 1 MHz to 1 GHz frequency range $\kappa_s^* \approx 4.4$ (Robinson 2004).

The real permittivity of the bulk pore fluid at low frequencies is much higher than that of sand particles because water molecules are dipolar molecules and they tend to rotate and line up with the external EM field. Energy is stored due to the directional alignment of water molecules. With increase of frequency, the rotation of water molecules becomes more and more difficult to keep up with the changes of the external field due to the impeding forces between water molecules. A lag between the rotation of water molecules and the reversion of the applied field results in a decrease in water real permittivity and an increase in water polarization loss, reflecting less energy storage and more energy dissipation. Further increase in frequency makes the rotation of water

molecules nearly impossible. As a result, the rotation of water molecules no longer contributes to the energy storage, and the real permittivity of water drops to a stable minimum value. The polarization loss drops to zero because no energy is dissipated without the rotation of water molecules. This change in water dielectric permittivity with frequency is termed the dielectric relaxation, and the frequency at which the polarization loss reaches its maximum is called the dielectric relaxation frequency.

If the behavior of water molecules is not affected by clay surface forces, they are called the free water molecules. The dielectric permittivity of the free water molecules κ_w can be well described by the Debye relaxation function (Kaatze 1996) as:

$$\kappa_w = \kappa'_{w,\infty} + \frac{\kappa'_{w,s} - \kappa'_{w,\infty}}{1 + j \cdot f / f_{w,rel}} \qquad [3.4]$$

where $\kappa'_{w,s}$ and $\kappa'_{w,\infty}$ are the pre-relaxation and post-relaxation real permittivities of the free water molecules and $f_{w,rel}$ is their relaxation frequency.

According to Friedman (1998), $\kappa'_{w,\infty}$ is approximately 5.5, and this value is almost unaffected by the temperature and pore fluid salinity. The salinity S is defined as the total mass of solid salts in grams dissolved in one kilogram of solution and expressed as parts per thousand (ppt). In contrast, the pre-relaxation real permittivity $\kappa'_{w,s}$, relaxation frequency $f_{w,rel}$ are affected by temperature and salinity. At a salinity less than 35 ppt, analytical solutions for $\kappa'_{w,s}$ and $f_{w,rel}$ as functions of salinity S (ppt) and temperature T (℃) were determined by Klein and Swift (1977) by fitting polynomial functions to the measured dielectric permittivities of NaCl solutions. The resulting equations are:

$$\kappa'_{w,s}(T,S) = \kappa'_{w,s}(T,0) \cdot a(T,S) \qquad [3.5]$$

$$f_{rel}(T,S) = \frac{f_{rel}(T,0)}{b(T,S)} \qquad [3.6]$$

in which $\kappa'_{w,s}(T,0)$ and $f_{rel}(T,0)$ are the pre-relaxation real permittivity and relaxation frequency of the deionized water:

$$\kappa'_{w,s}(T,0) = 87.134 - 1.949\times10^{-1}T - 1.276\times10^{-2}T^2 + 2.491\times10^{-4}T^3 \qquad [3.7]$$

$$f_{rel}(T,0) = \frac{1}{1.1109\times10^{-10} - 3.824\times10^{-12}T + 6.938\times10^{-14}T^2 - 5.096\times10^{-16}T^3} \qquad [3.8]$$

$$a(T,S) = 1.0 + 1.613\times10^{-5}TS - 3.656\times10^{-3}S + 3.210\times10^{-5}S^2 - 4.232\times10^{-7}S^3 \qquad [3.9]$$

$$b(T,S) = 1.0 + 2.282\times10^{-5}TS - 7.638\times10^{-4}S - 7.760\times10^{-6}S^2 + 1.105\times10^{-8}S^3 \qquad [3.10]$$

By combining equations [3.4], [3.5] and [3.6], the dielectric permittivities of free water molecules at different temperatures and salinities are calculated and plotted in Figure 3.2. It can be seen that the salinity has a very small influence on the dielectric permittivity of free water molecules if it is less than 10 ppt.

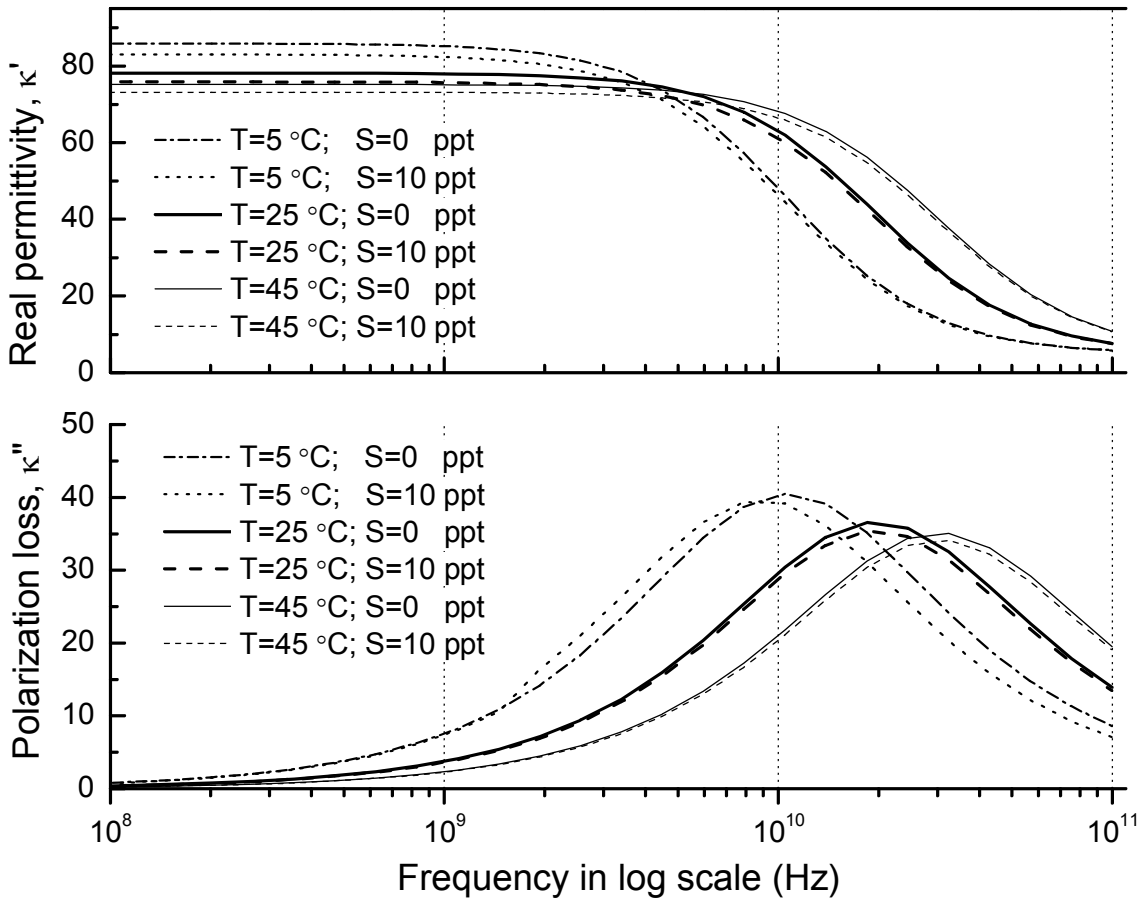

Figure 3.2 Dielectric permittivities of bulk pore fluid at different temperature and salinity according to equations [3.4] to [3.10]

An analytical expression relating the DC electrical conductivity of a pore fluid σ_{el} (S/m) to its salinity was established by Stogryn (1971) by fitting a polynomial function to the measured ionic conductivity of sea water (primarily NaCl) at a temperature of 25 ℃:

$$\sigma_{el} = S\left(0.18252 - 1.4619\times10^{-3}S + 2.093\times10^{-5}S^2 - 1.282\times10^{-7}S^3\right) \quad [3.11]$$

In most natural soils, the DC electrical conductivity of the bulk pore fluid σ_{el} rarely exceeds 1 S/m, which corresponds to a salinity of less than 5.7 ppt from equation [3.11]. At this low salinity, the real permittivity of the bulk pore fluid at 20 ℃ can be assumed to be a constant at frequencies less than 1 GHz: $\kappa_w^{'} \approx 79$.

For sand-water mixtures, it is reasonable to consider the water molecules in the bulk pore fluid as free water molecules because the specific surface area of sand particles is very small (much less than $1 m^2/g$) and the surface forces have little influences on the bulk pore fluid. Thus, the equivalent dielectric permittivity of the bulk pore fluid κ_{el}^* in sand-water mixtures can be determined by combining equation [3.4] and [3.11]:

$$\kappa_{el}^*(f) = \kappa_w - j\frac{\sigma_{el}}{2\pi f \varepsilon_0} \qquad [3.12]$$

3.2.3 Equivalent Dielectric Permittivity of Sand-Water Mixtures

Using the modified MG mixing formula (Equation [3.3]), the theoretical equivalent dielectric permittivity of a sand-water mixture at different volumetric water content θ and pore fluid DC electrical conductivity σ_{el} (S/m) are calculated and plotted in Figure 3.3. The imaginary component of the mixture equivalent dielectric permittivity κ_{mx}^* has been converted to the effective electrical conductivity σ_{eff} through equation [2.2] so that the variation of the DC electrical conductivity (approximated by σ_{eff} at low frequencies) with porosity can be more clearly demonstrated. In the calculation, sand particles were divided into equal fractions with each fraction equal to 5 percent and the number of

iteration M equals the number of fractions. The temperature of the bulk pore fluid was assumed to be 20 ℃.

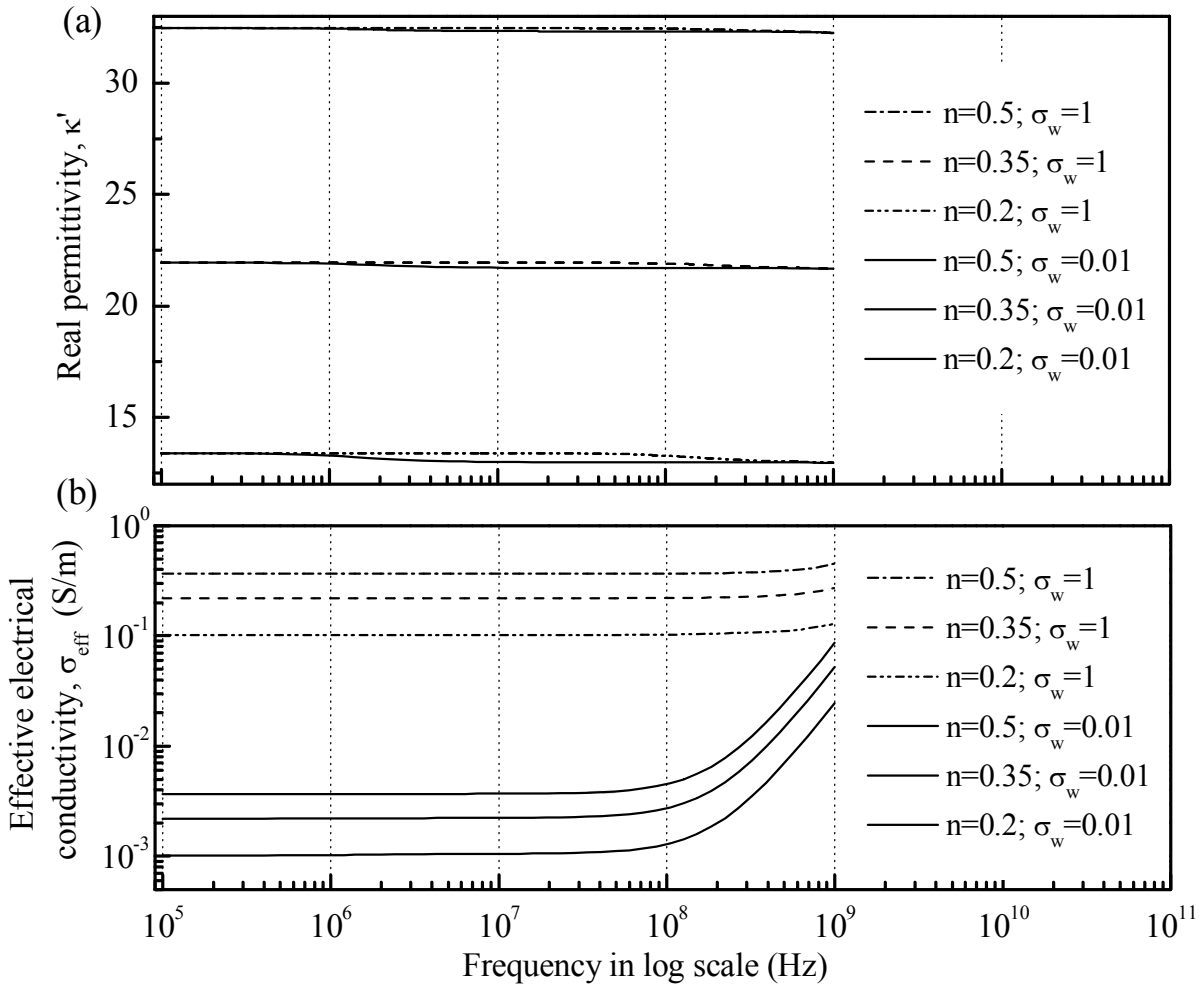

Figure 3.3 Dielectric spectrum of a sand-water mixture at different porosity and pore fluid DC electrical conductivity according to equations [3.3] and [3.12]

Figure 3.3a shows that the real permittivity of a sand-water mixture κ'_{mx} is nearly constant at frequencies less than 1 GHz and is barely affected by the pore fluid DC electrical conductivity σ_{el}. Two orders of increase in the pore fluid DC electrical

conductivity (from 0.01 to 1 S/m) only causes a very small variation in the real permittivity. This indicates that, in soils containing both sand and clay, the sand does not contribute to the dielectric dispersion, and the dielectric dispersion is solely caused by the presence of clay. On the other hand, the influence of volumetric water content θ on the mixture real permittivity is very obvious: a decrease in θ results in a decrease in the mixture real permittivity over the entire frequency range. When a soil is fully saturated, the volumetric water content θ is identical to the porosity n. Therefore, the porosity n is identified as the most important factor controlling the real permittivity of saturated sands.

The mixture effective electrical conductivity σ_{eff} is affected by both the volumetric water content θ and the DC electrical conductivity of the bulk pore fluid σ_{el} as shown in Figure 3.3b. A lower volumetric water content θ results in a lower effective electrical conductivity because the volume of conductive pore fluid is decreased. The increase in σ_{eff} at high frequency end (>100 MHz) is due to the polarization loss of the bulk pore fluid. At low frequencies (less than 1 MHz), the effective electrical conductivity of the mixture no longer changes with frequency because the contribution of the polarization loss to the effective electrical conductivity becomes very small. Thus the effective electrical conductivity at these frequencies can be treated as the DC electrical conductivity of the mixture σ_{mx}.

To investigate the relationship between the real permittivity and volumetric water content (porosity) of sand-water mixtures, the real permittivities of sand-water mixtures at 50 MHz were calculated using the modified MG mixing formula and compared with the measured real permittivities of saturated Hart sands at 50 MHz by Campbell (1990) as

shown in Figure 3.4a. This theoretical relationship between the real permittivity and volumetric water content applies for other pore fluid electrical conductivities less than 1 S/m and frequencies less than 1 GHz, because the influences of the pore fluid electrical conductivity and frequency have little impact on the real permittivity as demonstrated in Figure 3.3a. As a comparison, the real permittivities from the Polder-van Santen formula (equation [3.13]) and from the empirical correlation established by Wensink (1993) (equation [3.14]) are plotted. The Polder-van Santen formula, also named as the de Loor formula (de Loor 1968), is widely used in geophysics to calculate the real permittivity of a mixture from its components.

$$\theta \cdot \frac{\kappa_w^{'} - \kappa_{mx}^{'}}{\kappa_w^{'} + 2\kappa_{mx}^{'}} + (1-\theta) \cdot \frac{\kappa_s^{'} - \kappa_{mx}^{'}}{\kappa_s^{'} + 2\kappa_{mx}^{'}} = 0 \qquad [3.13]$$

$$\kappa_{mx}^{'} = 3.2 + 41.4\theta + 16\theta^2 \qquad [3.14]$$

where θ is the volumetric water content. It is equivalent to the porosity n if a soil is fully saturated.

Figure 3.4a shows that the real permittivity from the Polder-van Santen formula is consistently lower than the measured values. The empirical correlation by Wensink (1993) gives good estimation for the real permittivity at low porosities but tend to underestimate the real permittivity at medium to high porosities. Most natural sands have a porosity ranging from 0.2 to 0.5 (Terzaghi et al. 1996). Over this porosity range, the modified MG mixing formula gives better estimation for the real permittivity of sand-water mixtures than the other two correlations.

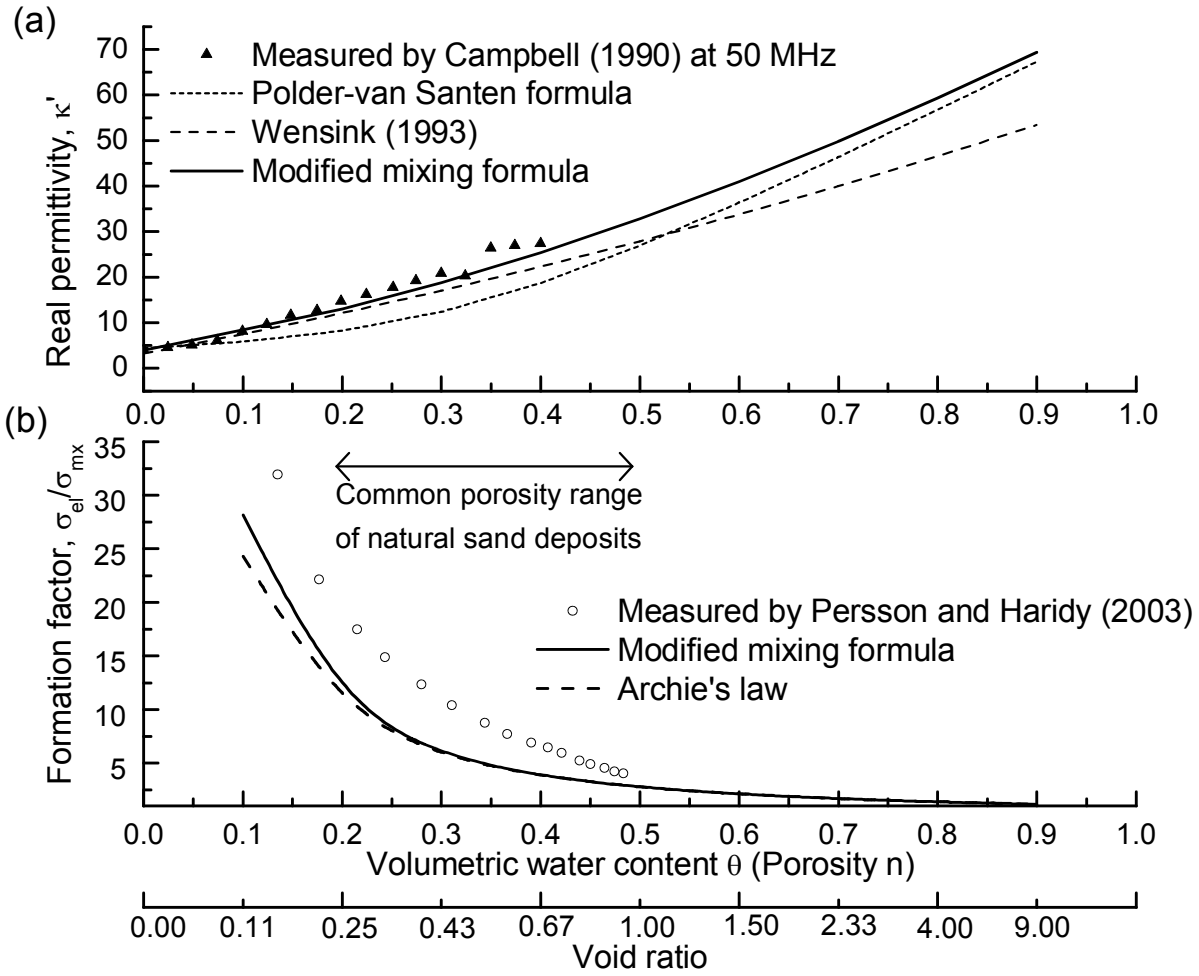

Figure 3.4 Equivalent dielectric permittivity of sand-water mixture as a function of porosity

To study the relationship between the porosity and DC electrical conductivity of sand-water mixtures, a formation factor F is frequently calculated by dividing the DC electrical conductivity of the bulk pore fluid σ_{el} by the DC electrical conductivity of the mixture σ_{mx}:

$$F = \sigma_{el} / \sigma_{mx} \qquad [3.15]$$

The effective electrical conductivity of the sand-water mixtures at 1 kHz was calculated using the modified MG mixing formula at a randomly chosen pore fluid DC

electrical conductivity of 0.1 S/m. Since the polarization loss no longer contributes to the effective electrical conductivity of the sand-water mixture at this low frequency, the calculated effective electrical conductivity was considered to be equal to the DC electrical conductivity of the mixture. Thus, the formation factor can be calculated and plotted as a function of porosity as shown in Figure 3.4b.

The formation factor can also be calculated by Archie's Law (Archie 1942):

$$F = n^{-p} \qquad [3.16]$$

where n is the overall porosity and p is the cementation factor (1.3 to 2 from Archie's tests). According to Dafalias and Arulanandan (1979b), the value of p should be 1.5 for spherical particles.

The theoretical formation factor from the modified MG mixing formula agrees very well with those from Archie's Law. The agreement between the formation factors from the two approaches is remarkable, given that these two approaches were derived on totally different bases.

The measured formation factor of the sand-water mixture by Persson and Haridy (2003), however, is higher than the predicted values by both Archie's law and the modified MG mixing formula. This might be because sand particles are not strictly spherical, and the non-spherical shape of sand particles tends to decrease the DC electrical conductivity of the mixture and then increases the formation factor.

3.2.4 Equivalent Dielectric Permittivity of Clay-Water Mixtures

The electromagnetic properties of clay-water mixtures are much more complicated than those of sand-water mixtures. Nevertheless, they can also be analyzed using the same framework as the sand-water mixtures and the modified Maxwell-Garnet formula as long as the equivalent dielectric permittivity of the clay inclusions can be correctly determined. Unlike sand particles, the equivalent dielectric permittivity of the clay inclusions is highly related to their structures. Thus several possible structures of common clay minerals are reviewed in the following analysis. Based on the review, a theoretical model is established for clay aggregates formed by stacked clay particles so that the equivalent dielectric permittivity of soils containing such clay aggregates can be investigated.

3.2.4.1 Review of Structures of Clay Minerals and Modeling

The most abundant clay minerals in natural soils are kaolinite, illite, and smectite. The surfaces of these clay minerals are usually negatively charged due to isomorphous substitution. Negatively charged clay surfaces are neutralized by an accumulation of cations in the proximity of the clay surfaces, forming the Stern and diffuse double layers (Mitchell and Soga 2005). These cations are usually referred to as counterions. The counterions affect the arrangement of clay particles through mediating the interactive forces between them. As clay particles become smaller and thinner, the surface forces begin to gain relevance to the body forces of clay particles and the type of counterions becomes more and more important. The structure of smectite minerals is especially

sensitive to the type of counterions and pore fluid electrolyte concentration because individual smectite plates are extremely thin (~9.5 Å). In the presence of divalent counterions such as Ca^{2+} and Mg^{2+}, the thin smectite plates usually stack up layer by layer to form stable clay aggregates because the attractive London-van der Waals forces and the ion correlation forces reach an equilibrium with the repulsive forces arising from the ion hydration, osmotic pressures and structural alteration of water molecules (Aylmore and Quirk 1971). A salient characteristics of these aggregates is that the basal spacing between two smectite plates in such an assembly is about 9.5 Å over a wide range of salt concentrations from distilled water to 1 molar $CaCl_2$ (Quirk 1986), corresponding to electrical conductivities from 10^{-6} to about 11.5 S/m (Santamarina et al 2001). Ca-illite particles form similar but weaker assemblies (Aylmore and Quirk 1971), probably because the illite particles have similar surface characteristics as smectite but they are thicker than smectite plates. Thus, the surface forces have less predominant influences on the behavior of illite particles. The aggregates do not form when the counterions are Na^+ and the salt concentration in the pore fluid is low. At salt concentrations less than 0.3 M NaCl (electrolyte electrical conductivity ≈ 3.2 S/m), the distance between smectite plates increases considerably, leading to a large swelling potential. Similar, though less significant swelling was also observed for Na-illite (Quirk and Murray 1991). Therefore, at an electrolyte electrical conductivity less than 1 S/m, the Ca-smectite and Ca-illite form aggregates as shown in Figure 3.5a while the Na-smectite and Na-illite are dispersed as shown in Figure 3.5b. When the pore fluid salt concentration is high, the clay aggregates can further associate face-to-edge or edge-to-

edge to form clay clusters as shown in Figure 3.5c. If no association between clay aggregates occurs, the soil is referred to be in a deflocculated state (Figure 3.5a).

Kaolinite particles are much thicker than smectite plates and illite particles. As a result, their arrangement is less sensitive to the type of counterions and electrolyte concentration. However, their arrangement is more sensitive to the pH value of the pore fluid because the particle edges can be positively or negatively charged, depending on the pH value, and the kaolinite particles have comparable edge and face surface areas. In an acid environment (low pH), the edges of kaolinite are usually positively charged and associated with the negatively charged particle faces to form clay clusters (van Olphen 1977) as shown in Figure 3.5d; In a basic environment, both the edges and faces are negatively charged and the kaolinite particles are totally dispersed as illustrated in Figure 3.5b.This effect of pH is much smaller for smectite and illite minerals because the face surface areas of these minerals is much larger than their edge surface areas and the edge potential is masked by the face diffuse double layer (Santamarina et al. 2001).

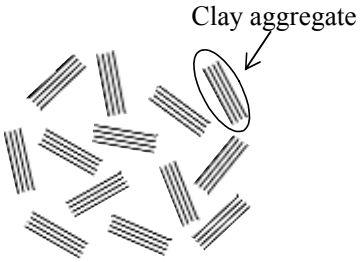

(a) Deflocculated clay aggregates (Ca-smectite and Ca-illite at low salt concentrations)

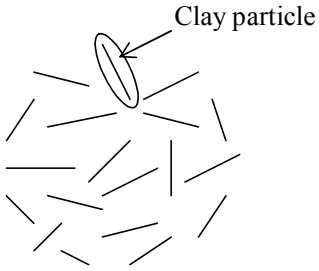

(b) Dispersed clay particles (Na-smectite, Na-illite or kaolinite in a basic environment);

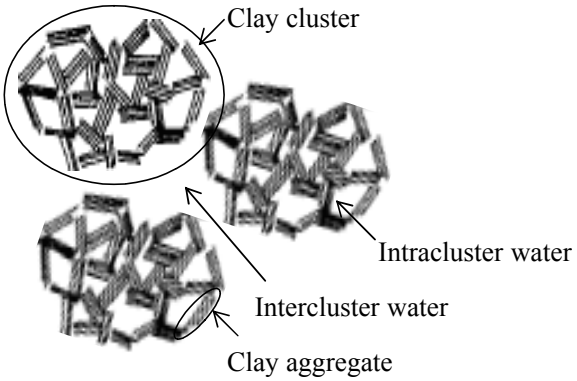

(c)) Flocculated clay aggregates (Ca-smectite and Ca-illite at high salt concentrations)

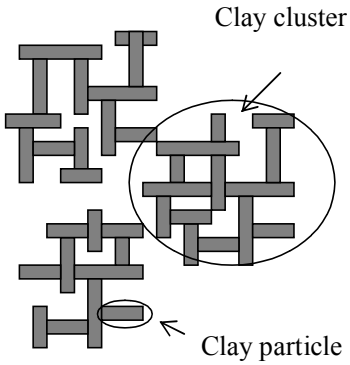

(d) Flocculated clay particles (kaolinite in a acid environment)

Figure 3.5 Schematic representations of the structures of important clay minerals: (a) deflocculated clay aggregates; (b) dispersed clay particles; (c) flocculated clay aggregates; (d) flocculated clay particles

3.2.4.2 An Oblate Spheroidal Model for Clay Aggregates

The clay aggregates shown in Figure 3.5a and 3.5c can be modeled as oblate spheroids composed of the alternate distribution of solid clay particle and intra-aggregate water layers as illustrated in Figure 3.6a, where all faces of the clay particles are perpendicular to the short major axis (a_z) of the aggregate. A shape factor R is defined as the ratio between the lengths of the long major axis L and the short major axis T:

$$R = L / T \qquad [3.17]$$

Spheroids are frequently used to model soil particles (e.g., Dafalias and Arulanandan 1979; Fricke 1953; Thevanayagam 1993; Wobschall 1977) because they provide a flexibility to mathematically characterize particles with various shapes. Depending on the value of R, a spheroid can exhibit a platy (R>>1), a spherical (R=1) or a needle-like (R<<1) shape. However, the previous studies assumed that the spheroids are electromagnetically isotropic, which may not be true for clay aggregates as will be shown in the following analysis.

The dispersed clay particles in Figures 3.5b and 3.5d can be considered as special clay aggregates sandwiched by external bound water layers without internal water layers as shown in Figure 3.6b. Thus, the model creates a flexible framework for analyzing the electromagnetic properties of clay minerals in various particle arrangements.

The equivalent dielectric permittivity of a soil containing such aggregates is determined in three steps:

1. EM properties of clay particles and intra-aggregate pore fluid;
2. EM properties of clay aggregates at different orientations;
3. EM properties of a soil-water system containing such clay aggregates.

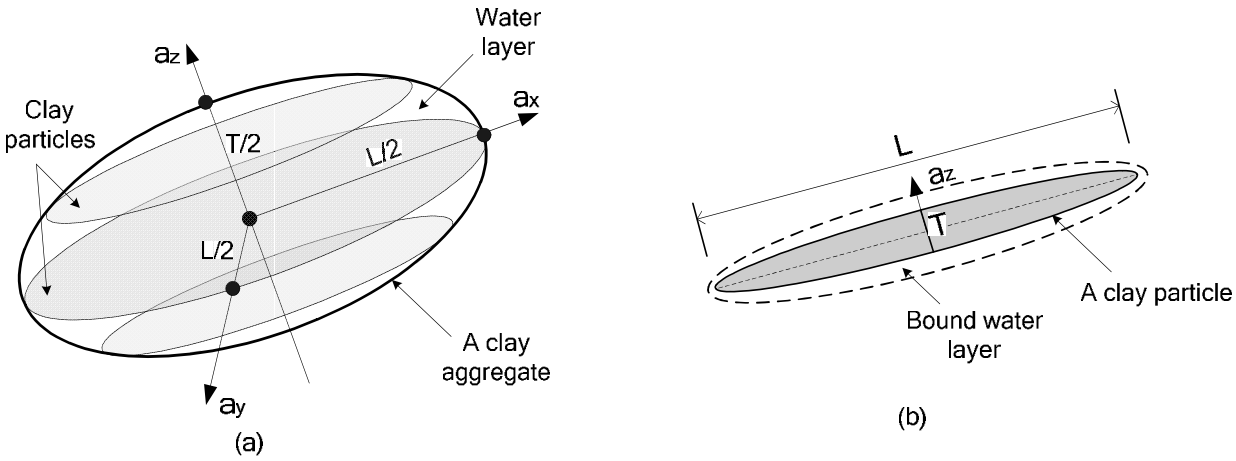

Figure 3.6 Modeling of clay inclusions: (a) a spheroidal clay aggregate composed of alternate distribution of clay particles and intra-aggregate water layers; (b) a clay particle coated by external bound water layers

In this study, the intra-aggregate pore fluid refers to the water molecules confined in clay aggregates and the water molecules adsorbed to the external surfaces of clay particles. Accordingly, the bulk pore fluid are assumed to be unaffected by clay surface forces.

3.2.4.3 EM properties of solid clay particles and intra-aggregate pore fluid

(1) Solid clay particles

At frequencies less than 1 GHz, the dielectric permittivities of solid clay particles are constant. For example, the real permittivity k' is 5.1 for kaolin, 5.8 for illite and 5.5 for smectite and the polarization losses k'' of these clay minerals are negligible (Robinson 2004). The solid clay particles can be considered as nonconductive because the movements of ions through the mineral crystal lattice are negligible as compared with

their movements through aqueous electrolytes. However, most clay particles exhibit a surface conductance in the presence of water because of the existence of the adsorbed Stern and diffuse double layers in the proximity of clay surfaces. This surface conductance may develop only in the direction parallel to clay faces.

(2) Intra-aggregate pore fluid

In the proximity of clay surfaces, the electromagnetic properties of water molecules are strongly affected by clay surface forces. These water molecules are called the bound water molecules. The first three molecular layers of water from clay surfaces are usually considered as bound water and the average thickness of each layer d_w is about 3 Å (Friedman 1998), an estimate slightly higher than the diameter of one water molecule (2.8 Å). Therefore, the thickness of the entire bound water layer is about 9 Å. Beyond this distance, the surface forces have very small influences on the EM properties of water molecules.

Assume that the frequency-dependent dielectric permittivity of the *i*th molecular layer of bound water $\kappa_{bw}(i)$ can also be characterized by the Debye relaxation function:

$$\kappa_{bw}(i) = \kappa'_{bw,\infty} + \frac{\kappa'_{bw,s}(i) - \kappa'_{bw,\infty}}{1 + j\dfrac{f}{f_{rel}(i)}} \qquad [3.18]$$

where $\kappa'_{bw,s}(i)$ and $f_{rel}(i)$ are the pre-relaxation real permittivity and dielectric relaxation frequency of the *i*th bound water molecular layer; $\kappa'_{bw,\infty}$ is the post-relaxation real permittivity of the bound water molecules. After relaxation, the real permittivities of

all the bound water layers drop to the same minimum value as that of free water molecules, $\kappa'_{bw,\infty}$ = 5.5 (Saxon 1952). However, both $\kappa'_{bw,s}(i)$ and $f_{rel}(i)$ are different from those of free water molecules.

A relationship between the real permittivity of water molecules and the distance of water molecules from the solid clay surface *x* (Å) was proposed by Friedman (1998):

$$\kappa'_{bw}(x) = \kappa'_{w,\infty} + \left(\kappa'_{w,s} - \kappa'_{w,\infty}\right)(1 - e^{-x}) \qquad [3.19]$$

where $\kappa'_{w,s}$ and $\kappa'_{w,\infty}$ are the pre-relaxation and post-relaxation real permittivity of free water molecules. The proposed equation fits well with the real permittivities of bound water molecules measured by Thorp (1959). However, the frequency range over which the equation [3.19] is applicable was not explicitly specified by Friedman (1998). Since the measurements by Thorp (1959) were performed at a frequency of 0.5 MHz and the bound water relaxation is generally considered to occur over the 1 MHz to 1 GHz frequency range, it is appropriate to consider that the calculated real permittivity from equation [3.19] corresponds to the pre-relaxation real permittivity of bound water molecules. Based on this equation, the average pre-relaxation real permittivity of the first, second and third bound water layers $\kappa'_{bw,s}(n)$ are determined to be 62, 76 and 78 by assuming their distances from clay surfaces are 1.5 Å, 4.5 Å and 7.5 Å, respectively.

Bound water molecules also have lower relaxation frequencies than free water molecules. Or and Wraith (1999) derived an equation to calculate the relaxation frequencies of bound water layers by combing the Debye (1929) model and the viscosity profile of water layers by Low (1976). From their analysis, the relaxation frequencies of

the n*th* bound water layers $f_{rel}(n)$ are 100 MHz, 500 MHz, 1.5 GHz when n equals to 1, 2 and 3, respectively.

As previously discussed, the distance between two adjacent clay particles in an aggregate is about 9.5 Å, which is a distance of about 3 water molecular layers. Since the intra-aggregate water molecules are subjected to the surface forces from two adjacent clay particles, the average dielectric permittivity of the intra-aggregate pore fluid κ_{ip} can be calculated by averaging the dielectric permittivities of the first and second bound water layers using equation [3.20]. For dispersed clay particles, three molecular layers of bound water are attached to both sides of a clay particle. Therefore, m in equation [3.20] should be three for individual clay particles and two for clay aggregates.

$$\kappa_{ip} = \sum_{i=1}^{m} \left(\kappa'_{bw,\infty} + \frac{\kappa'_{bw,s}(i) - \kappa'_{bw,\infty}}{1 + j\dfrac{f}{f_{rel}(i)}} \right) / m \qquad [3.20]$$

The dielectric permittivities of three bound molecular water layers and the average dielectric permittivity of the intra-aggregate pore fluid (m=2) are plotted in Figure 3.7. Also plotted is the dielectric permittivity of the bulk pore fluid at a temperature of 20 ℃ for comparison purpose. Here, the effects of counterions on the dielectric permittivity of bound water molecules are not considered for lack of information.

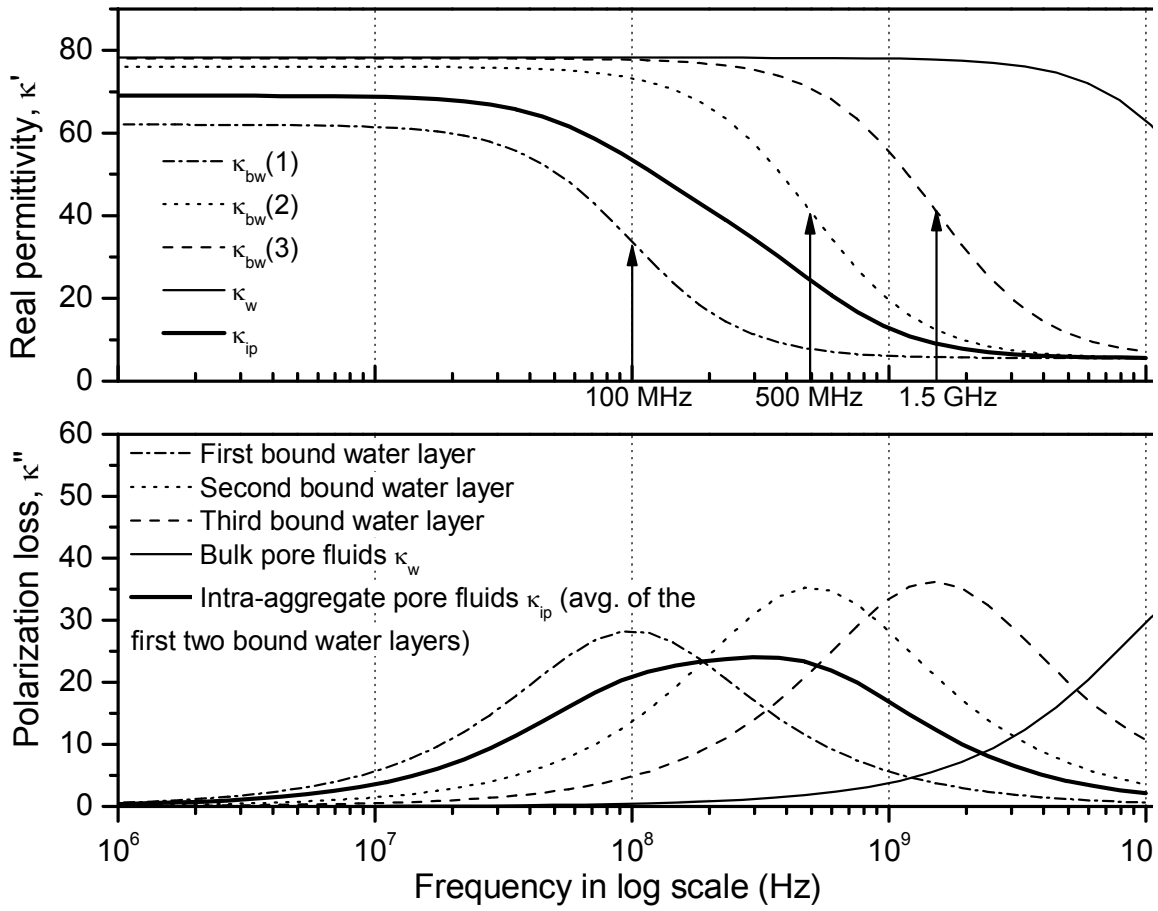

Figure 3.7 Dielectric permittivities of bound water layers, free water and intra-aggregate pore fluid

(3) Electrical conductivity of intra-aggregate pore fluid

The counterions accumulated in the proximity of clay surfaces may move freely in the direction parallel to clay surfaces and thus provide an extra electrical conductance for the intra-aggregate pore fluid, which is termed the *surface conductance*. The surface conductance may arise from the counterions in both the Stern and the diffuse double layers (Leroy and Revil, 2004). The movements of counterions in the direction normal to clay surfaces, however, can be hindered due to the strong attractive forces of the surfaces.

The electrical conductivities of intra-aggregate pore fluid in the directions tangential and normal to the clay surface are schematically illustrated by Figure 3.8, in which t_0 is the distance beyond which the electrical conductivity of the pore fluid is no longer affected by clay surface forces. The average distance between clay particles in a clay aggregate is less than this distance.

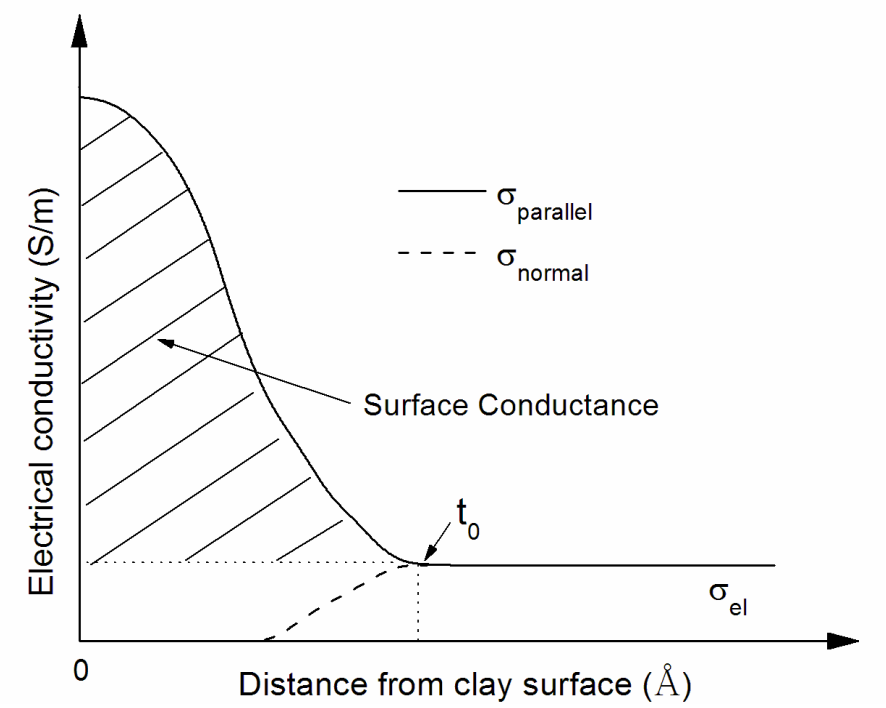

Figure 3.8 Illustration of the electrical conductance of intra-aggregate pore fluid

In the direction tangential to the clay surfaces, the electrical conductivity of the aggregate σ_T can be calculated using the following equation (Santamarina et al 2001):

$$\sigma_T = n_p \sigma_{el} + \left(1 - n_p\right) \cdot \rho_s \cdot \lambda_s \cdot S_a \qquad [3.21]$$

in which n_p = intra-aggregate porosity $= t_w / (t_w + t_p)$ [3.22]

where t_w and t_p are the average thicknesses of the intra-aggregate water layer and clay particles (m); ρ_s = mass density of the solid clay particles (kg/m^3); λ_s = surface conductance (S); S_a = total specific surface area (m^2/kg) = the ratio between the surface area of a particle and its mass. σ_{el} is the electrical conductivity of the bulk pore fluid (S/m).

For very thin clay particles, the average thickness t_p is related to the total specific surface area (Santamarina et al. 2002) by:

$$t_p = \frac{2}{\rho_s \cdot S_a} \qquad [3.23]$$

Thus, the intra-aggregate porosity is primarily determined by the total specific surface area S_a because the average thickness of intra-aggregate pore fluid t_w in an aggregate is approximately 9.5 Å and the mass density of solid clay particles can be roughly estimated ($\approx 2.65\times10^3$ kg/m^3):

$$n_p = \frac{t_w}{t_w + \frac{2}{\rho_s \cdot S_a}} \qquad [3.24]$$

If the pore fluid DC electrical conductivity σ_{el} is less than 1 S/m, the first term in equation [3.21] can be dropped because its contribution to σ_T is much less than that of the second term regardless of the specific surface area. Therefore, equation [3.21] can be rewritten as:

$$\sigma_T = \frac{2\lambda_s}{t_w + \frac{2}{\rho_s \cdot S_a}} \qquad [3.25]$$

The surface conductance λ_s can be estimated from the cation exchange capacity (CEC) of the clay, the mobility of counterions u_{cat} $(m^2V^{-1}s^{-1})$ and the total specific surface area S_a (santamarina et al. 2001) as:

$$\lambda_s \approx \frac{u_{cat} \cdot CEC}{S_a} \qquad [3.26]$$

The cation exchange capacity (CEC) is usually defined as the quantity of exchangeable cations (milliequivalent) per 100 grams of dry clay. An equivalent contains 6.02×10^{23} electron charges or 96,500 Coulombs. The estimated surface conductance of the most common clay minerals from equation [3.26] and the intra-aggregate porosity n_p from equation [3.24] are listed in Table 3.1. In the above calculation, it is assumed that the counterions are Ca^{2+} with a mobility of $6.2 \times 10^{-8} m^2V^{-1}s^{-1}$ (value from Santamarina et al. 2001).

The surface conductance in Table 3.1 is calculated on the assumption that the u_{cat} has a value equal to the mobility of Ca^{2+} in a dilute pore fluid, which may overestimate the mobility of the ions in the Stern layer and diffuse double layer because the ions are more concentrated and restrained in these layers. The actual mobility of Ca^{2+} and the corresponding surface conductance can be lower. If the same value of surface conductance is assigned for all minerals, the σ_T of a clay aggregate is uniquely determined by the total specific surface area as shown in Figure 3.9.

Table 3.1 Estimated surface conductance and intra-aggregate porosity of major clay minerals (Data from Mitchell and Soga, 2005)

Clay Minerals	CEC (meq/100g)	Total Specific Surface, S_a (m^2/g)	Estimated surface conductance λ_s (S)	Shape of individual clay particle, R	Intra-aggregate porosity, n_p (for t_w = 9.5 Å)
Smectite	80-150	700-840	4.7×10^{-9} - 1×10^{-8}	100 - 1000	0.47 - 0.51
Illite	10-40	65-100	5×10^{-9} - 3×10^{-8}	~ 10	0.07 - 0.11
Kaolinite	3-15	10-30	3.75×10^{-8}- 3.75×10^{-7}	3 - 10	0.01 - 0.04
Vermiculite	100-150	870	5.8×10^{-9}- 9×10^{-9}	100 - 1000	0.52

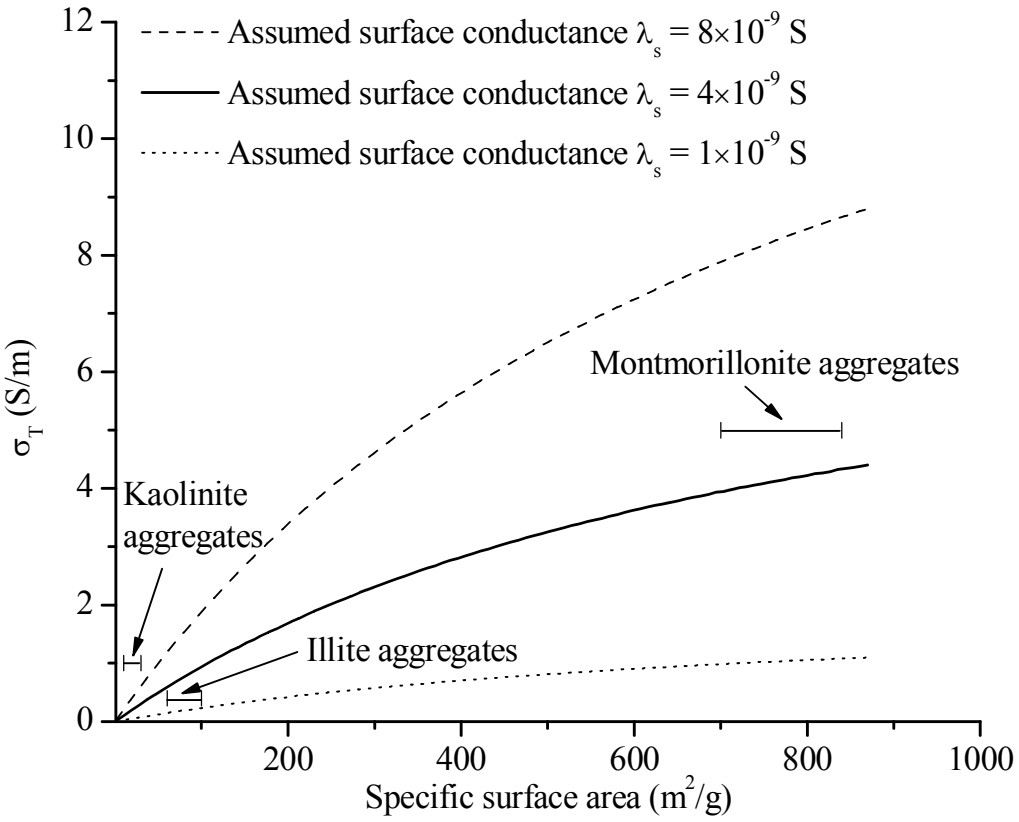

Figure 3.9 DC electrical conductivity of clay aggregates as a function of specific surface area in the direction parallel to clay faces

Figure 3.9 shows that the electrical conductivity of a smectite aggregate is approximately four times as much as that of an illite aggregate and about eight times as much as that of a kaolinite particle in the direction parallel to the clay surfaces under the assumption that the surface conductance is the same.

In the direction normal to the clay surface, the DC electrical conductivity of intra-aggregate pore fluid is assumed to be equal to that of the bulk pore fluid σ_{el}. The actual value can be lower but is not important because its influences on the effective dielectric permittivity of the aggregate is very small, which will be illustrated in the following section.

3.2.4.4 EM properties of clay aggregates

The equivalent dielectric permittivity of a clay aggregate depends on its orientation with respect to the external EM fields. For an oblate spheroidal aggregate, its orientation is uniquely determined by the orientation of its short major axis a_z because the spheroid is axisymmetric along a_z. In the polar coordination system, the orientation of a_z is defined by two angles: the azimuthal angle δ and angle ϕ as illustrated in Figure 3.10, where ϕ is the angle between a_z and the Z axis and δ is the angle between the positive X axis and the projection of a_z on the XY plane. The angle δ can vary from 0 to 2π and ϕ from 0 to π.

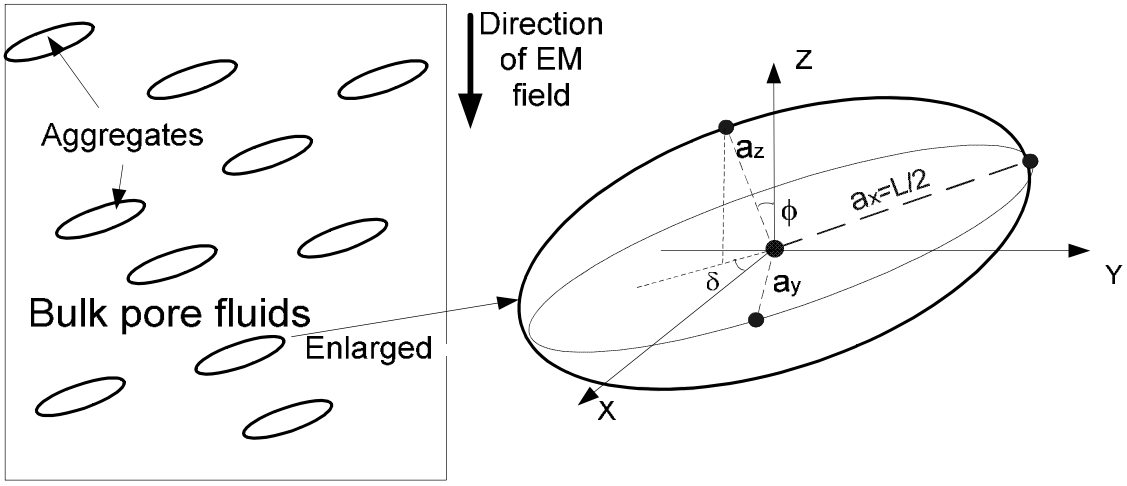

Figure 3.10 Orientation of an oblate spheroidal particle (inclusions) in the medium uniquely determined by two angles

(a) EM properties of the aggregate at two special orientations

Without losing generality, it is assumed that the external EM field is directed in the Z direction. The EM properties of an aggregate in this direction are a function of the angle ϕ. Two special orientations are (1) the short major axis a_z parallel to the external field (ϕ = 0 or π) as shown in Figure 3.11a and (2) a_z perpendicular to the external field ($\phi = \pi/2$) as shown in Figure 3.11b. The equivalent dielectric permittivity of the aggregate in both orientations can be analyzed using the equivalent circuits.

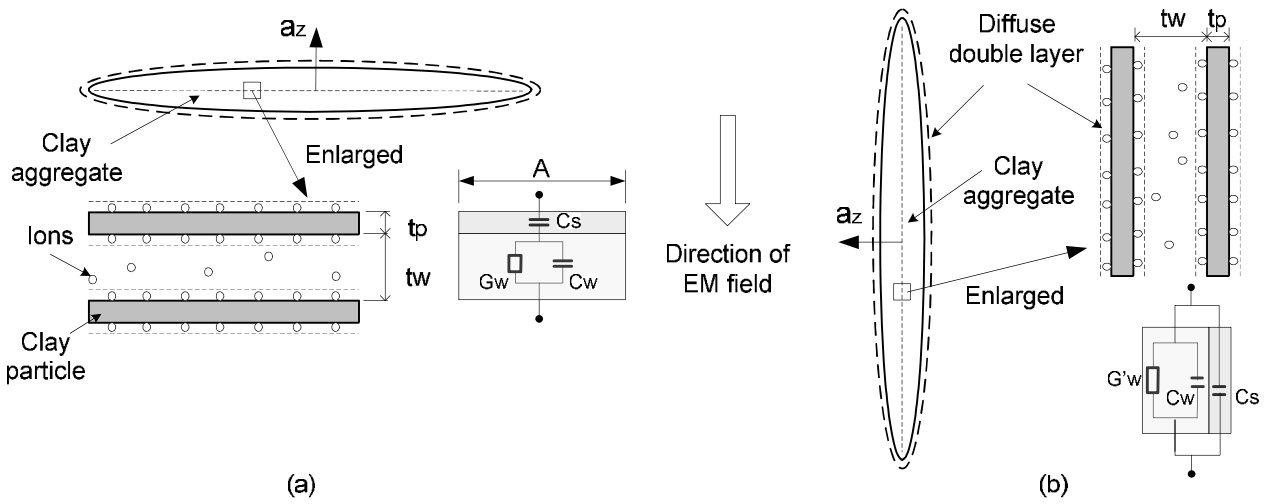

Figure 3.11 Two special orientations of a clay aggregate with respect to the external EM field: (a) Short major axis a_z parallel to external EM field; (b) a_z perpendicular to the external EM field

When the short major axis a_z is parallel to the external EM field ($\phi = 0$), the aggregate can be modeled as a capacitor C_S in series connection with a capacitor C_W and a conductor G_W, where C_S represents the capacitance of the solid clay particle, C_W represents the capacitance of the intra-aggregate pore fluid and G_W represents the conductance of the intra-aggregate pore fluid:

$$C_S = \kappa_s^{'} \varepsilon_0 \frac{A}{t_p} \qquad [3.27]$$

$$C_W = \kappa_{ip}^{'} \varepsilon_0 \frac{A}{t_w} \qquad [3.28]$$

$$G_W = \left(\kappa_{ip}^{"} + \frac{\sigma_{el}}{2\pi f \varepsilon_0} \right) \frac{A}{t_w} \qquad [3.29]$$

in which A is the width of the aggregate; $\kappa_s^{'}$ is the real permittivity of the solid clay particle (~5); $\kappa_{ip}^{'}$ and $\kappa_{ip}^{"}$ are the real permittivity and polarization loss of the intra-aggregate pore fluid, whose values can be calculated by equation [3.20]; σ_{el}, ε_0, f, t_p and t_w are previously defined.

The equivalent dielectric permittivity of such a combination, κ_N^*, was derived by Hilhorst (1998) as:

$$\kappa_N^* = \frac{1}{\dfrac{n_p}{\kappa_{ip}^{'} - j\left(\kappa_{ip}^{"} + \dfrac{\sigma_{el}}{2\pi f \varepsilon_0} \right)} + \dfrac{1 - n_p}{\kappa_s^{'}}} \qquad [3.30]$$

where n_p is the intra-aggregate porosity of the aggregate. It is related to the total specific surface area by equation [3.24]. It should be noted that equation [3.30] does not include the electrical conductance contributed by the external surface of the clay aggregate. According to Weiler (1968), this contribution is approximately equal to λ_s / A, where A is the width of a clay aggregate. The width of a clay aggregate A is usually larger than 1 μm (Mitchell and Soga 2005). As a result, the contribution of external surfaces to the electrical conductivity of the clay aggregate will be less than 0.01 S/m because the surface conductance λ_s is less than 10^{-8} S (refer to Table 3.1), which is small enough to be neglected.

When a_z is perpendicular to the EM field as shown in Figure 3.11b ($\phi = \pi/2$), the spheroid can be modeled as parallel connection of C_S, C_W and $G_W^{'}$, in which $G_W^{'}$ represents the combined pore fluid conductance and surface conductance; C_S and C_W are previously defined. The equivalent dielectric permittivity of such a combination is:

$$\kappa_T^* = n_p \cdot \left(\kappa_{ip}^{'} - j \cdot \kappa_{ip}^{''}\right) + \left(1 - n_p\right) \cdot \kappa_s^{'} - j \frac{\sigma_T}{2\pi f \varepsilon_0} \qquad [3.31]$$

in which, σ_T is calculated from equation [3.25], other parameters are defined previously. In this case, the contribution of external surfaces for the electrical conductivity of the aggregate has already been included because the total surface area is used to calculate σ_T.

The theoretical dielectric spectra of smectite and illite aggregates from equations [3.30] and [3.31] are plotted in Figure 3.12. In the calculation, the specific surface area of the smectite and illite minerals are assumed to be 780 m^2/g and 80 m^2/g. Therefore, their intra-aggregate porosities n_p are 0.5 and 0.09 from equation [3.24] for an average intra-aggregate water layer thickness t_w of 9.5 Å. The surface conductance of both clay minerals λ_s is assumed to be 1×10^{-9} S. The DC electrical conductivity of the bulk pore fluid σ_{el} is assumed to be 0.01 S/m.

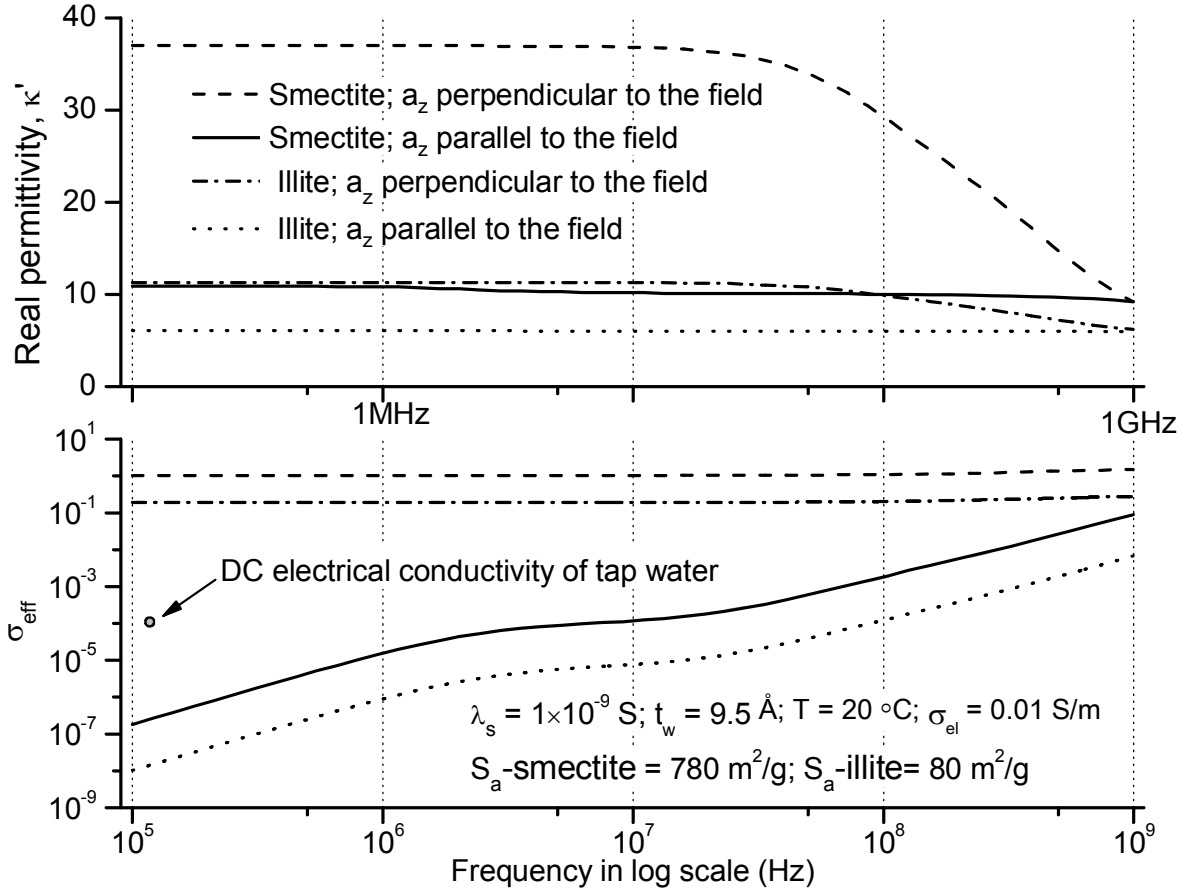

Figure 3.12 Dielectric spectra of aligned clay aggregates

The upper plot of Figure 3.12 shows that, in the direction perpendicular to the clay faces (i.e. a_z parallel to the EM field), the real permittivity of an aggregates is low and close to that of solid clay particles, indicating that the high real permittivity of the intra-aggregate water layers is masked by the confining clay particles with low real permittivity, a situation also observed by Friedman (1998). When a_z is perpendicular to the external field, the real permittivity of the aggregate at low frequencies is significantly higher than that in the previous orientation because the water layers are directly exposed to the external field. The drop in the real permittivity at frequencies higher than 10 MHz in the second case is due to the bound water relaxation. At 1 GHz, the real permittivities

of smectite aggregates in both orientations are close to 10 even though about half volume of the aggregate is water.

The lower plot of Figure 3.12 demonstrates that the aggregate is almost nonconductive when a_z is parallel to the external field because the solid clay particles block the electrical current flow in this direction. When a_z is perpendicular to the external field, the effective electrical conductivity is several orders higher than that in the first case due to the surface conductance. Therefore, the electromagnetic anisotropy of the clay aggregates is more related to their anisotropy in electrical conductivity rather than in dielectric permittivity.

(b) Short major axis a_z randomly oriented

When a_z is neither parallel nor perpendicular to the external field, the EM property of the aggregate can be analyzed by decomposing the external field in the Z direction into two components: E_T perpendicular to a_z and E_N parallel to a_z as shown in Figure 3.13.

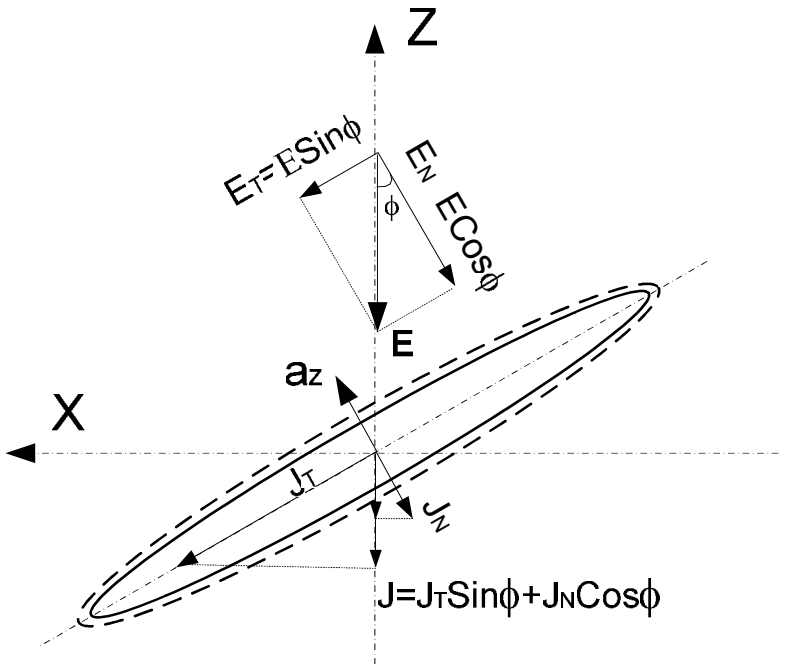

Figure 3.13 Equivalent current caused by the external field

The current densities caused by E_T and E_N are:

$$J_T = \sigma_T E_T = \sigma_T E \cdot Sin\phi \qquad [3.32]$$

and

$$J_N = \sigma_N E_N = \sigma_N E \cdot Cos\phi \qquad [3.33]$$

Thus, an equivalent DC electrical conductivity in the direction of the EM field can be derived as:

$$\sigma_\phi = \frac{J_N Cos\phi + J_T Sin\phi}{E} = \sigma_N \cdot \cos^2\phi + \sigma_T \cdot \sin^2\phi \qquad [3.34]$$

This equation indicates that $\sigma_\phi = \sigma_N = \sigma_T$ if the aggregate is electrically isotropic. For large specific surface area minerals, σ_N is much less than σ_T as shown in Figure

3.12. As a result, $\sigma_\phi \approx \sigma_T \cdot \sin^2 \phi$, whose maximum value is reached when $\phi = \pi / 2$ and minimum value is zero when $\phi = 0$ *or* π. Since σ_T is determined by the specific surface area and surface conductance and the surface conductances of several important clay minerals are close as shown in Table 3.1, the total specific surface area is identified as the most important factor determining the electrical conductivity of an aggregate.

The same derivation can also be applied for the dielectric permittivity. As a result, an equivalent dielectric permittivity in the Z direction can be expressed as

$$\kappa_\phi^* = \kappa_N^* \cdot \cos^2 \phi + \kappa_T^* \cdot \sin^2 \phi \qquad [3.35]$$

where κ_N^* is from equation [3.30] and κ_T^* is from equation [3.31].

3.2.4.5 EM properties of a soil containing clay aggregates

A soil containing clay aggregates can be modeled as a two-phase mixture of spheroidal clay aggregates and the bulk pore fluid and the electromagnetic property of the mixture can also be determined using the modified MG mixing formulas (equation [3.3]) as a sand-water mixture. However, the equivalent dielectric permittivity of the inclusions κ_{in}^* is no longer a constant but a function of the aggregate orientation, whose value can be calculated by equation [3.35]. Moreover, the depolarization N is no longer 1/3 but dependent on the shape and orientation of the aggregate.

(a) Depolarization factor

Analytical solutions for the depolarization factor N were derived by Fricke (1953) when the EM field is directed in line with one of the three major axes of a spheroid. The depolarization factor in the direction of the short major axis is:

$$N_0 = \frac{1+e^2}{e^3}\left(e - \tan^{-1} e\right) \qquad [3.36]$$

The depolarization factor in the direction perpendicular to the short major axis is determined accordingly from equation [3.37] because the sum of the depolarization factors in three mutually perpendicular directions should be one and the depolarization factors along two long major axes are the same for an oblate spheroid.

$$N_{\pi/2} = (1 - N_0)/2 \qquad [3.37]$$

in which $e = \sqrt{R^2 - 1}$ and $R = L/T$,

where L and T are the lengths of the long and short major axes of the oblate spheroid. The ratio R characterizes the shape of the spheroid and corresponds to the ratio between the width and thickness of an aggregate. When L = T, $N_0 = N_{\pi/2} = \frac{1}{3}$, which are the depolarization factors for spheres.

A more complicated case is that the short major axis a_z rotates in a vertical plane, for example in the XZ plane ($\delta = 0$ plane) as shown in Figure 3.13. The depolarization factor in the Y direction is independent of the angle ϕ because one of the long major axes is always in line with the Y direction:

$$N_Y = N_{\pi/2} \qquad [3.38]$$

The depolarization factors in the X and Z directions are functions of the angle ϕ and should have values between N_0 and $N_{\pi/2}$. Assume the depolarization factor along the Z direction can be expressed as:

$$N_Z(\phi) = N_0 \cdot g(\phi) + N_{90} \cdot f(\phi) \qquad [3.39]$$

where $f(\phi)$ and $g(\phi)$ are random functions of angle ϕ.

Then, the depolarization factor in the X direction can be defined accordingly because of symmetricity:

$$N_X(\phi) = N_0 \cdot f(\phi) + N_{90} \cdot g(\phi) \qquad [3.40]$$

They are subjected to the following limiting conditions:

$$\begin{cases} N_X + N_Z + N_Y = 1 \\ N_X(\pi/2) = N_0 \quad N_X(0) = N_{\pi/2} \\ N_Z(\pi/2) = N_{\pi/2} \quad N_Z(0) = N_0 \end{cases} \qquad [3.41]$$

which lead to

$$\begin{cases} f(\phi) + g(\phi) = 1 \\ f(\pi/2) = 1 \quad f(0) = 0 \\ g(\pi/2) = 0 \quad g(0) = 1 \end{cases} \qquad [3.42]$$

A simple assumption for *f* and *g* based on the above limitations is

$$\begin{cases} f(\phi) = \sin^2 \phi \\ g(\phi) = \cos^2 \phi \end{cases} \qquad [3.43]$$

Then

$$\begin{cases} N_X(\phi) = N_0 \cdot \sin^2\phi + N_{\pi/2} \cdot \cos^2\phi \\ N_Z(\phi) = N_0 \cdot \cos^2\phi + N_{\pi/2} \cdot \sin^2\phi \\ N_Y = N_{\pi/2} \end{cases} \quad [3.44]$$

Similar to the modeling of sand-water mixtures, the clay aggregates are assumed to be added to the bulk pore fluid in a step-wise manner. For sand-water mixtures, the iteration process is adopted for the purpose of addressing the interferences among densely packed sand particles. For clay-water mixtures, the iteration process also serves the purpose of addressing the electromagnetic anisotropy of the clay aggregates. At each step, the small portion of clay aggregates at the same orientation is added to the bulk pore fluid because they have the same equivalent dielectric permittivity and the same depolarization factor. The resulting equivalent dielectric permittivity is treated as a new medium for further addition of the aggregates oriented at other orientations.

(b) Anisotropic clay-water mixture

Under high over-burden pressures, it is possible that almost all clay aggregates become parallelly oriented to form an anisotropic clay-water mixture, so the EM properties of the mixture are different in the vertical and horizontal directions. When the modified MG mixing formula is applied, the equivalent dielectric permittivity of the inclusions $\kappa_{in}^* \equiv \kappa_N^*$ and the depolarization factor $N \equiv N_0$ in the vertical direction. In the horizontal direction, $\kappa_{in}^* \equiv \kappa_T^*$ and $N \equiv N_{\pi/2}$. Without any aggregates, the initial equivalent dielectric permittivity of the mixture is equal to that of the bulk pore fluid $\kappa_{en,0}^* = \kappa_{el}^*$. The theoretical equivalent dielectric permittivity of an anisotropic illite-water

mixture is calculated for both directions and plotted in Figures 3.14. The porosity of the mixture was assumed to decrease from 0.4 to 0.2. Typical values of the specific surface area S_a, surface conductance λ_s and shape factor R of illite are assumed in the calculation: S_a = 80 m^2/g, $\lambda_s = 1\times10^{-9}$ S and R = 10. A pore fluid electrical conductivity σ_{el} of 0.01 S/m and a temperature of 20 ℃ were also assumed.

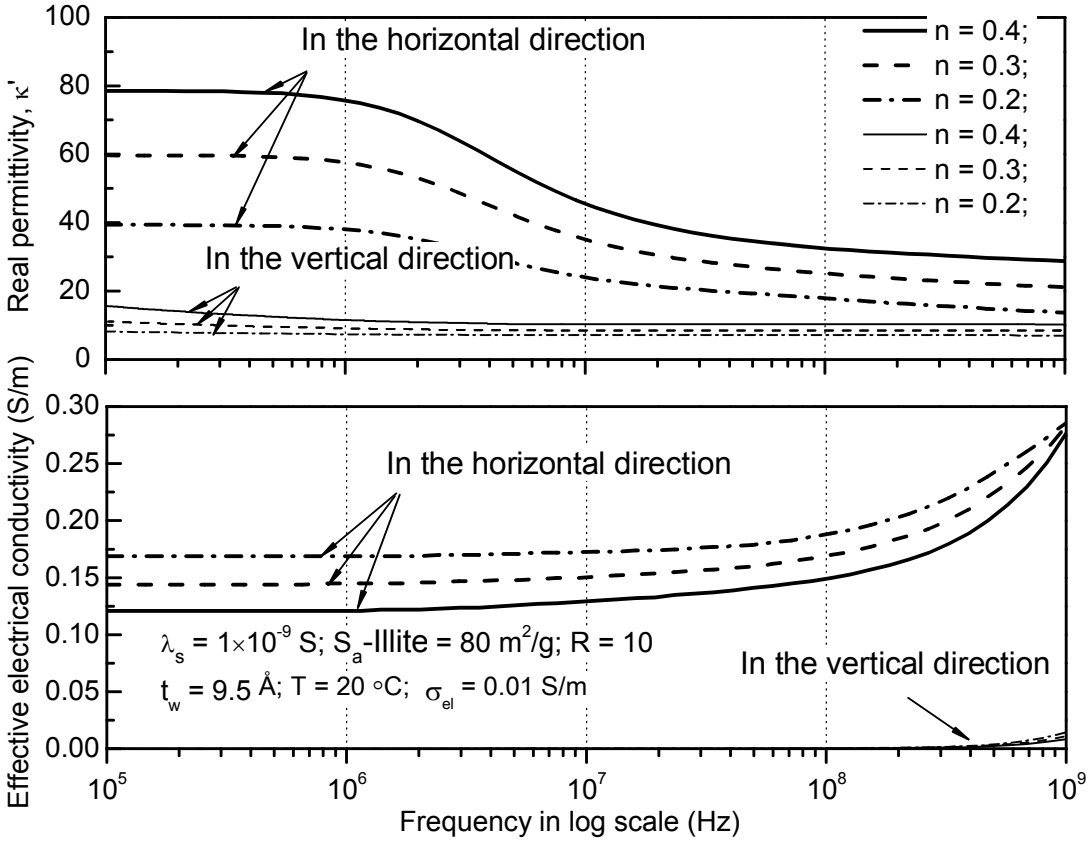

Figure 3.14 Equivalent dielectric permittivity of an anisotropic mixture in the vertical and horizontal directions

The upper plot of Figure 3.14 demonstrates that the real permittivity is higher in the horizontal direction than in the vertical direction regardless of the porosity. The dielectric

dispersion behavior in the horizontal direction is also more significant than in the vertical direction because the DC electrical conductivity of the aggregate in the horizontal direction is much larger than that of the bulk pore fluid, which causes interfacial polarization.

The DC electrical conductivity of the mixture (approximated by σ_{eff} at low frequencies) in the vertical direction is very small and barely seen in the lower plot of Figure 3.14. The DC electrical conductivity of the mixture in the horizontal direction is related to the porosity. A lower porosity leads to a higher DC electrical conductivity of the mixture because the volumetric fraction of clay aggregates with high electrical conductivities increases with decreasing porosity. This is a tendency opposite to that of sand-water mixtures, for which DC electrical conductivity of the mixture decreases with decreasing porosity.

(c) Isotropic clay-water mixture

At high porosities, the aggregates can be randomly oriented, leading to an isotropic soil mass. Since an oblate spheroid can be uniquely represented by its short major axis a_z, a discussion on the orientation of the aggregates can be substituted by a discussion on the orientation of the short major axis a_z.

For an isotropic mixture, the angle ϕ between a_z and the Z axis in any vertical plane (e.g., the XZ plane, $\delta = 0$) should be evenly distributed from 0 to π. Moreover, the possibility that a_z is located in the XZ plane should be statistically the same as the possibility that it is located in the XY and YZ planes. Since the direction of the X axis

can be randomly defined in the horizontal plane, the above argument applies for any other vertical planes ($\delta \neq 0$). Therefore, the calculation for the mixture equivalent dielectric permittivity can be simplified to the case where one third of short major axes a_z are located in the XZ plane, one third in the YZ plane and one third in the XY plane. The contribution of each portion of clay aggregates to the overall equivalent dielectric permittivity of the mixture can be calculated using the modified mixing formula. When the short major axes of the clay aggregates are evenly distributed in the XZ plane, their contribution to the mixture equivalent dielectric permittivity in the Z direction can be calculated using equation [3.3] because the effective dielectric permittivities and depolarization factors of these aggregates as a function of angle ϕ have been derived (equations [3.36] and [3.44]). The spheroidal aggregates with short major axes in the YZ plane contribute equally to the mixture equivalent dielectric permittivity in the Z direction as do the aggregates with short major axes in the XZ plane. When the contribution of the aggregates with their short major axes in the XY plane is calculated, $\kappa_{in}^{*} \equiv \kappa_{T}^{*}$ and $N_i \equiv N_{\pi/2}$ because the major short axes of these aggregates are always perpendicular to the Z direction.

3.2.5 Application of the model to clay mixtures

The dielectric spectra of three clay-water mixtures – calcium bentonite, sodium bentonite and kaolinite – are analyzed using the theoretical model. Bentonite is a soil with a very high percentage of smectite minerals. The dielectric spectra of the sodium bentonite-water and kaolinite-water mixtures were measured over the frequency range from 20 MHz to 1.3 GHz using a Hewlett-Packard HP-8752A network analyzer in

conjunction with a HP-85070A dielectric coaxial termination probe. The system was calibrated by measuring the impedances of air (open circuit), metallic shorting block (short circuit), and deionized water. More details of the measuring system are given in Chapter 5. The dielectric spectrum of the calcium bentonite-water mixture was measured by Rinaldi and Francisca (1999) using a Hewlett-Packard HP4191A impedance analyzer over the frequency range from 1 MHz to 1 GHz. Some physical properties of these mixtures are listed in Table 3.2. The specific surface areas of the sodium bentonite and kaolinite were measured using the ethylene glycol monoethyl ether (EGME) adsorption method. The details of the EGME adsorption method can be found in Cerato and Lutenegger (2002).

Table 3.2. Some physical properties of the mixtures being studied

	Specific surface area	Liquid limit (%)	Plastic limit (%)	Specific gravity	Volumetric water content (%)	Sources
Ca-bentonite	-	250	50	2.65	89	(Rinaldi and Francisca 1999)
Na-bentonite	670	840	170	2.72	92.4	This study
Kaolinite	35	37	15	2.65	55.7	This study

The clay particles or aggregates in these mixtures are considered to be randomly oriented because of the high porosities of the mixtures. Nine parameters are involved in the theoretical modeling of an isotropic clay-water mixture. They are the dielectric permittivity of solid clay particle κ_s, dielectric permittivity of the intra-aggregate pore fluid κ_{ip}, dielectric permittivity of the bulk pore fluid κ_{el}, total specific surface area of the clay mineral S_a, intra-aggregate porosity n_p, total porosity of the mixture n, pore fluid electrical conductivity σ_{el}, surface conductance of the clay mineral λ_s and the

shape factor of the clay aggregate R. The values of κ_s of several clay minerals are very close (~5). The value of κ_{el} can be determined from equation [3.4] at a specific temperature T. The values of κ_{ip} can be determined from equation [3.20], in which m = 2 for clay aggregates and m = 3 for individual clay particles because three molecular water layers are attached to each side of a clay particle. The total specific surface area S_a can be directly measured or estimated from Table 3.1. From the total specific surface area and the average thickness of intra-aggregate water layer t_w, the intra-aggregate porosity n_p can be calculated using equation [3.24]. For the kaolinite and Na-bentonite, the intra-aggregate porosity actually refers to the volumetric fraction of bound water molecules attached to the external surface of individual kaolinite and bentonite particles because one particle is considered as a special aggregate where no internal water layers exist. The predetermined parameters for three mixtures are listed in Table 3.3. All mixtures are assumed to be fully saturated so that the volumetric water content is identical to the total porosity. Therefore, there are only three undetermined parameters for each mixture: bulk pore fluid electrical conductivity σ_{el}, surface conductance λ_s and shape factor R. These parameters can be back-calculated by fitting the theoretical model to the measured dielectric spectra. The numerical optimization was performed using MATLAB function *fmincon*. The criterion for optimization was taken to be that the optimized parameters yield a minimum sum for the absolute differences between the calculated and measured equivalent dielectric permittivities over the entire frequency range. Both the measured and optimized theoretical dielectric spectra are shown in Figure 3.15. The optimized parameters are also listed in Table 3.3.

Table 3.3 Predetermined and optimized parameters for three clay-water mixtures

	Parameters used in modeling								
	Predetermined values						Optimized values		
	S_a (m^2/g)	t_w (Å)	n_p	κ_s	m	T (°C)	σ_{el} (S/m)	λ_S (S)	R
Ca-bentonite	780*	9.5	0.5	5.5	2	20	0.031	7.6×10^{-9}	62
Na-bentonite	670	2×9.5	0.66	5.5	3	20	0.014	8.7×10^{-9}	161
Kaolinite	35	2×9.5	0.08	5.5	3	20	0.044	1.1×10^{-9}	3

- Estimated value

The optimized surface conductances of the Ca-bentonite and Na-bentonite are close and both of them are located in the range estimated from the cation exchange capacity (CEC) in Table 3.1. A slightly lower surface conductance of Ca-bentonite than Na-bentonite indicates that the clay surfaces are more conductive when the clay particles are totally dispersed than confined in the aggregates. The back-calculated surface conductance of kaolinite is lower than the estimated values from CEC, but it agrees with the value determined by Leroy and Revil (2004), which ranges from 1×10^{-9} to 2×1^{-9} S depending on the pore fluid salinity. The ratio between the width and thickness of individual smectite plates usually ranges from 100 to 1000 (Mitchell and Soga 2005). The shape factor of Na-bentonite particles (R=156) is located in this range. The shape factor of the Ca-bentonite aggregates is lower than 100 because the smectite aggregates have similar width as but larger thickness than individual smectite particles. The optimized value of 62 is a reasonable estimation for Ca-bentonite. The optimized R for kaolinite is 3, which is in the range estimated for kaolinite minerals. For the mixture of Ca-bentonite and water, a slight mismatch between the modeled and measured real permittivity at lower frequencies is most likely due to the electrode polarization (Klein and Santamarina

1997), which usually results in the measured real permittivity being higher than the actual real permittivity at frequencies lower than 10 MHz.

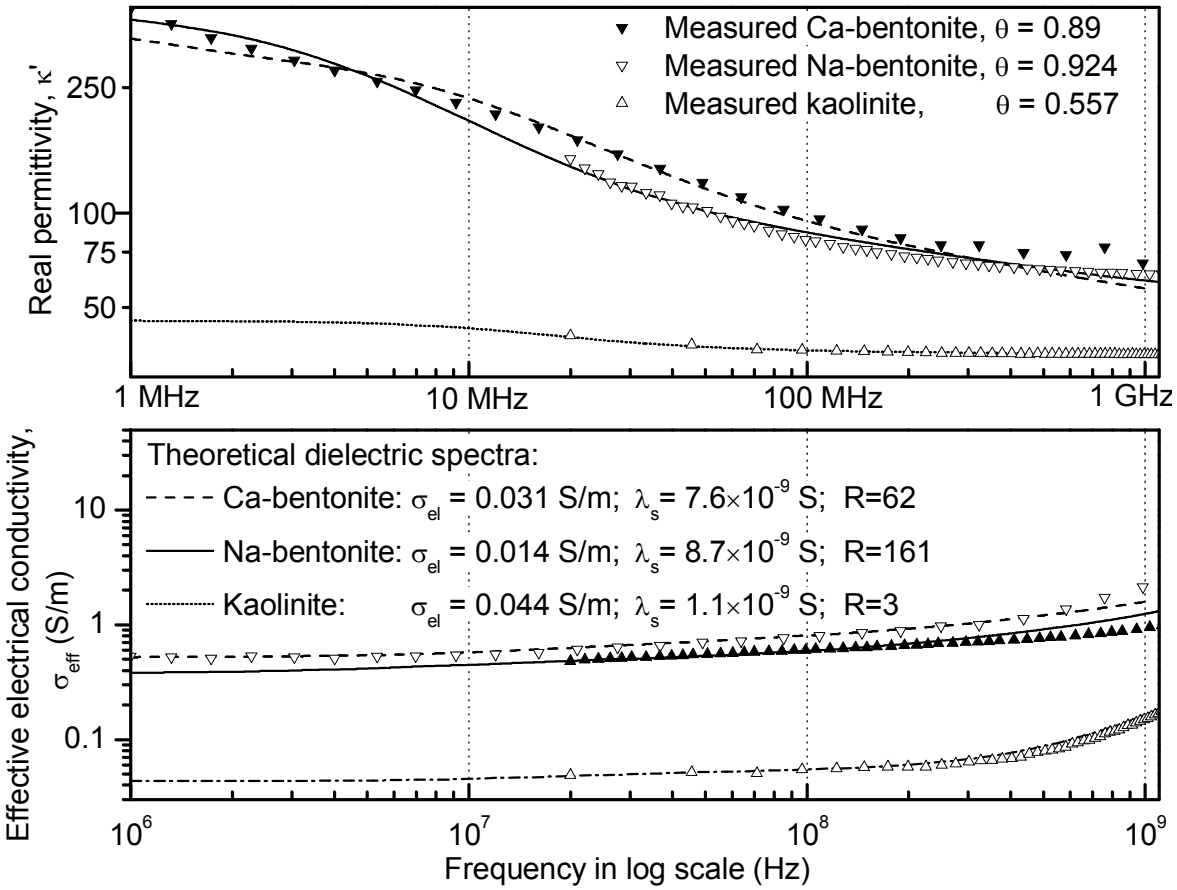

Figure 3.15 Theoretical and measured dielectric spectra of saturated bentonite and kaolinite

3.2.6 Mechanism of dielectric dispersion

Over the 1 MHz to 1 GHz frequency range, both interfacial polarization and bound water polarization affect the dielectric spectrum of fine-grained soils and the two mechanisms are coupled. The relative importance of each mechanism to the equivalent dielectric permittivity of a soil can be evaluated by assuming that one mechanism does not exist. Interfacial polarization is induced because the clay aggregates have higher

electrical conductivity than the bulk pore fluid and the high electrical conductivity of the clay aggregates is attributed to the surface conductance of clay minerals. Thus, interfacial polarization can be considered as nonexistent if the surface conductance of clay minerals is assumed to be zero. Similarly, bound water polarization affects the dielectric spectrum because the bound water molecules relax at lower frequencies than free water molecules. If the bound water molecules are assumed to have the same equivalent dielectric permittivity as the free water molecules, the effects of bound water polarization can be considered as nonexistent. The calcium bentonite-water mixture is used as a reference material to evaluate the influences of these two mechanisms. The optimized dielectric spectrum for it is replotted in Figure 3.16 together with two theoretical curves under the condition that either interfacial polarization or bound water polarization does not exist. For comparison purpose, the theoretical dielectric spectrum of a sand-water mixture at the same porosity and bulk pore fluid electrical conductivity is also plotted. Sand particles are assumed to be spherical in the calculation.

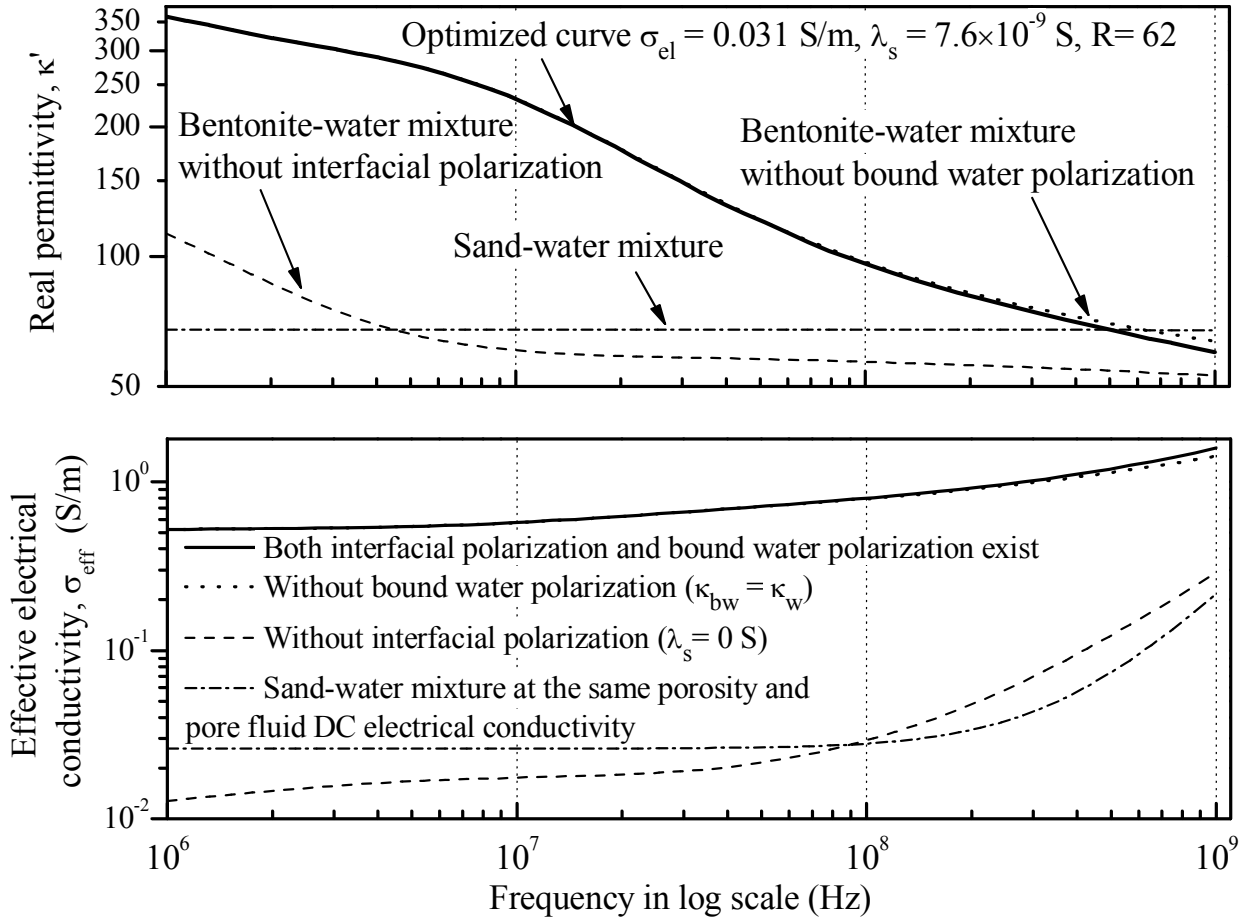

Figure 3.16 Importance of interfacial polarization and bound water polarization for dielectric dispersion behavior

It can be seen from Figure 3.16 that the interfacial polarization is the most important mechanism leading to the high dielectric dispersion and high electrical conductivity of the mixture. Without interfacial polarization, the real permittivity of the calcium bentonite-water mixture would be much smaller than the actually measured values and even smaller than that of sand-water mixtures because the platy shape of clay aggregates tends to decrease the real permittivity. The dielectric dispersion magnitude would also be small even for bentonite with the highest specific surface area. Moreover, interfacial polarization can affect the dielectric spectrum at frequencies as high as 1 GHz, contrary

to the common belief that the interfacial polarization is no longer effective above 200 MHz. Bound water polarization also contributes to the dielectric dispersion of the smectite-water mixture at high frequencies but its effect is minor compared with that of interfacial polarization.

The effective electrical conductivity σ_{eff} at low frequencies would be very small without the contribution of surface conductance because the platy aggregates tend to block the flow of the DC electrical current through the pore fluid. However, σ_{eff} increases to values higher than that of sand-water mixtures at high frequencies because of the bound water polarization loss, which is negligible for sand-water mixtures.

3.2.7 Discussion

(1) Depolarization factor

When the short major axis of a spheroidal particle is neither parallel nor perpendicular to the external EM field, the depolarization factor was assumed to vary from N_0 to $N_{\pi/2}$ according to equation [3.43]. Other assumptions for $f(\phi)$ and $g(\phi)$ can also be made. For example, a linear variation also satisfies all the limiting conditions, i.e., $f(\phi)=\frac{\phi}{(\pi/2)}$ and $g(\phi)=1-\frac{\phi}{(\pi/2)}$. However, it was found that two assumptions yield similar optimization results for both the bentonite-water and kaolinite-water mixtures, indicating that the model is not very sensitive to the selection of specific functions as long as these functions satisfy all the limiting conditions specified in equation [3.42].

(2) Surface conductance

In the theoretical model, the counterions on both the internal and external surfaces of clay aggregates are assumed to be able to move along the surface of clay particles. This assumption is confirmed by the optimized value of the smectite surface conductance. If the counterions on the internal surfaces of the aggregates were not movable, the optimized surface conductance would have to be several times larger than the currently calculated value to cause the same degree of dielectric dispersion. However, a surface conductance several times larger than the currently calculated value will be far out of the range estimated from the cation exchange capacity.

3.3 Conclusions

A physically based model is established to analyze the dielectric spectra of soils containing clay minerals. All parameters in the model have well-defined physical meanings and can be independently measured. The model creates a framework through which the coupled effects of interfacial polarization and bound water polarization on soil equivalent dielectric permittivity can be analyzed. The model fits well with the measured dielectric spectra of the sand-water, bentonite-water and kaolinite-water mixtures. Most importantly, the back-calculated values of the compositional and structural parameters of these soils agree very well with the values estimated from the mineralogical analysis.

Interfacial polarization is identified as the most important mechanism contributing to the dielectric dispersion behavior of fine-grained soils over the 1 MHz and 1 GHz frequency range. The magnitude of dielectric dispersion due to interfacial polarization is

controlled by the difference in electrical conductivity between the bulk pore fluid and clay aggregates. The electromagnetic properties of clay aggregates or particles are anisotropic: both the real permittivity and DC electrical conductivity are the highest in the direction tangential to the clay surfaces and the lowest in the direction normal to them. The maximum DC electrical conductivity of a clay particle or clay aggregate is determined by the total specific surface area and surface conductance of the clay mineral. Although the dielectric dispersion behavior can also be affected by bound water polarization, the contribution of bound water is relatively small as compared with that of interfacial polarization. The dielectric dispersion caused by the bound water polarization is also strongly related to the total specific surface area because the total specific surface area determines the intra-aggregate porosity of a soil, which characterizes the amount of bound water. Given the fact that the surface conductance varies in a narrow range for common clay minerals, the specific surface area is identified as the most important factor determining the electrical conductivity of clay aggregates and the dielectric dispersion behavior of fine-grained soils.

The influences of compositional, structural and environmental factors on the dielectric spectrum of clay will be discussed in the next chapter using the theoretical model.